20 May 2020

Prediction On Service Life Of Concrete Pipeline Buried In Chlorinated Environment Under Nonuniformly Distributed Earth Pressure

Lin Li

Weibing Gong
Missouri University of Science and Technology, weibing.gong@mst.edu

Jingpei Li

Construction and Building Materials 243 (2020) 118162

Contents lists available at ScienceDirect

Construction and Building Materials

journal homepage: www.elsevier.com/locate/conbuildmat

Prediction on service life of concrete pipeline buried in chlorinated environment under nonuniformly distributed earth pressure

Lin Li [a], Weibing Gong [b,*], Jingpei Li [b]

[a] Department of Civil and Environmental Engineering, Louisiana State University, Baton Rouge, LA 70803, USA
[b] Department of Geotechnical Engineering, Tongji University, Shanghai 200092, China

HIGHLIGHTS

- Service life of pipeline in chlorinated soil considers nonuniform earth pressures.
- Nonhomogeneous coefficient is introduced to describe pressure nonuniformity.
- Service life is shortened with increase of pressure nonuniformity and stress level.
- Thicker protective cover and shallower buried depth can extend service life.

ARTICLE INFO

Article history:
Received 12 October 2019
Received in revised form 3 January 2020
Accepted 12 January 2020
Available online 28 January 2020

Keywords:
Chlorinated soil
Service life
Diffusion
Corrosion
Nonuniform earth pressure
Underground concrete pipeline

ABSTRACT

This paper proposes an analytical model to estimate the service life of concrete pipelines buried in chloride contaminated soils, which properly considers the effects of nonuniformly distributed earth pressures on both the internal tensile stress of concrete protective cover and the chloride diffusion coefficient through the nonhomogeneous coefficient of earth pressure. It is assumed that the underground concrete pipeline arrives at the service life end when cracking induced by expansion pressure due to the corrosion products occurs in the concrete protective cover. Hence, the whole service life of underground concrete pipeline is composed of chloride diffusion period and protective cover corrosion period. The diffusion of chloride ions is simulated through a diffusion model for dual compound media and the service life of this period is evaluated by solving the diffusion equation. The service life of corrosion period is estimated based on the corrosion expansion pressure with the aid of the concrete tensile strength. The validity of chloride diffusion model is examined through the comparison between the present analytical analysis and the numerical analysis from finite element simulations, guaranteeing that there are reliable results available for the subsequent analysis of corrosion period. Comprehensive parametric studies are conducted to explore the effects of nonuniformly distributed earth pressures and concrete cover thickness on the pipeline service life. The results demonstrate that the nonuniformly distributed earth pressures lead to the occurrence of tensile stress in the protective cover and give rise to the increase in the chloride diffusion coefficient, which in fact accelerates the diffusion of chloride ions in the concrete pipeline and induces the cracking of concrete protective cover and thus significantly shortens the service life of concrete pipelines buried in chlorinated environment.

1. Introduction

With increasingly high requirements on the structure service life, the durability problem grows cumulatively serious and has turned into a significant research topic for practitioners and researchers in both industry and academia [1–7]. The underground concrete pipeline, as a primary concrete structure for cablecasting and water and oil delivery, suffers from more complex durability problem, because of more complex corrosion mechanism and load condition (i.e. nonuniformly distributed earth pressures). Among the factors that impair the durability of underground concrete pipelines in coastal regions, the chloride ion contamination takes the dominant place, because in coastal regions the soil is chronically immersed by sea water and the chloride ion content is always at a comparatively high level. When concrete pipelines are buried in the chlorinated environment, chloride ions will diffuse into the

* Corresponding author.
E-mail addresses: lli1@lsu.edu (L. Li), 12weibing_gong@tongji.edu.cn (W. Gong), lijp2773@tongji.edu.cn (J. Li).

https://doi.org/10.1016/j.conbuildmat.2020.118162
0950-0618/

concrete and gradually accumulate around steel bars, which will further give rise to the generation of rust. With the increase of rust, the corrosion expansion pressure increases and may bring about the concrete cracking. As the cracking develops to a certain degree, the concrete pipeline can be damaged, which may cause the pollution of soil and water due to pollution leakage and even give rise to the collapse of roads and houses because of the soil erosion around the pipeline. These potential adverse results will definitely cause great threat to people's life and safety. Therefore, to ensure that underground concrete pipelines can be safely put into the use in coastal regions for a long term, great attention should be paid to the prediction on the service life of underground pipelines in chlorinated soils.

Compared with the corrosion mechanism of concrete superstructures, the corrosion mechanism of underground concrete pipelines shows great difference. This is because underground concrete pipelines not only suffer from the attack of chloride ions, but also are under the influence of nonuniformly distributed earth pressures. It is without doubt that the nonuniformly distributed earth pressures affect the stress state of pipeline and thus exert great influences on the chloride diffusion in the concrete pipeline and the cracking of concrete protective cover. As a consequence, particular concern should be given when referring to common concrete structures to carry on researches to explore the durability problem of underground concrete pipelines. Up to now, extensive researches have been conducted to investigate the chloride diffusion behaviour in concrete structures with different loading levels. For example, Konin et al. [8] conducted several chloride diffusion tests on concrete specimens with different compressive strengths, which are in compressive states and under a sequence of drying and wetting circles. The test results yielded a relationship between the loading level and the chloride diffusion coefficient and indicate that the chloride diffusion rate in the concrete increases remarkably as the tensile stress level increases; Fransoic and Maso [9], Gowripalan et al. [10] and Castel et al. [11] carried on different experiments to investigate the chloride diffusion behaviour in the flexural concrete members and summarized that the diffusion rate of chloride ions in the tensile zone is much rapider than the rate in the compressive zone; Lim et al. [12] explored the chloride permeability of concrete slides subjected to the uniaxially compressive stress and observed that as the uniaxially compressive stress lies in a certain range, the chloride diffusion rate slows down slightly as the stress increases, whereas the chloride diffusion rate increases apparently as the uniaxially compressive stress exceeds the certain range; and Lu et al. [13] conducted chloride penetration experiments on concrete specimens subjected to axially compressive stress and statistically summarized the semi-empirical relationship between the stress level and the chloride diffusion rate. However, from the abovementioned researches, it is easily found that most of the investigations on the chloride diffusion behaviour in the concrete are based on the experiments conducted on concrete specimens, but they are lack of the theoretical analysis; moreover, the concrete specimens adopted in the experiments are in the plate form and the corresponding experimental results are unable to be directly applied to the exploration on the durability problem of underground concrete pipelines, since most underground concrete pipelines are circular.

Under the earth pressures, the stress and strain are generated within the underground concrete pipeline, which gives rise to the variation in the void ratio and the stress state of concrete. The relevant research [14] indicates that the chloride diffusion rate is highly related to the void ratio and stress state of concrete, and thus the earth pressures can exert influence on the chloride diffusion in the underground concrete pipeline. Furthermore, as the underground concrete pipeline is subjected to nonuniformly distributed earth pressures, there is compressive or tensile state at different locations within the pipeline. The void ratio of concrete increases and the microcracks get development when the concrete is in the tensile state, and hence the tensile state greatly accelerates the chloride diffusion in the pipeline; on the contrary, the compressive state results in the decrease of void ratio of concrete and further slows down the chloride diffusion [11,13]. Simultaneously, the stress state of underground concrete pipeline in the period of cracking due to corrosion expansion is also influenced when the pipeline is subjected to nonuniformly distributed earth pressures. As a consequence, it is of great significance to build an analytical model to estimate the service life of underground concrete pipelines under nonuniformly distributed earth pressures in chlorinated soils, based on the chloride diffusion theory as well as the theory on protective cover cracking caused by corrosion expansion.

To achieve this aim, the whole service life of concrete pipeline buried in chlorinated soils is divided into the diffusion period of chloride ions together with the cracking period of concrete protective cover. Both periods incorporate the effects of nonuniformly distributed earth pressures via introducing the nonhomogeneous coefficient of earth pressure. The chloride diffusion is modelled through the diffusion model for a dual compound media and the service life of this period is evaluated by deriving an analytical solution to the diffusion equation. The service life of corrosion period is predicted by means of corrosion expansion pressure along with the concrete tensile strength. The validity of proposed model for chloride diffusion is examined by finite element simulations, which ensures that the diffusion results are reliably available for the subsequent corrosion analysis. Comprehensive parametric studies are carried on to investigate the effects of nonuniformly distributed earth pressures and concrete cover thickness on the pipeline service life. The corresponding results are expected to provide significant guidance for designing underground concrete pipelines with adequate service life in chlorinated soils.

2. Chloride diffusion in underground concrete pipeline

2.1. Stress distribution of underground concrete pipeline

When the concrete pipeline is buried in the soil at a relatively shallow depth, the earth pressure acting on the pipeline in the vertical direction differs from that in the lateral direction. This degree of difference can become obvious as the buried depth decreases. The nonuniformly distributed earth pressures not only change the void ratio and stress state of concrete, but also give rise to the tensile zone in the underground pipeline, which definitely affects the chloride diffusion in the pipeline as well as the cracking of concrete protective cover. This indicates that the whole service life of underground concrete pipeline is under the great influence of nonuniformly distributed earth pressures. Therefore, the effects of nonuniform earth pressure on underground concrete pipeline should be taken into account. For the simplicity of building the analytical model, it is reasonable to decompose the nonuniformly distributed earth pressures into the lateral earth pressure, G_h, and the vertical earth pressure, G_v, respectively [15], which is shown in Fig. 1(a). The nonhomogeneous coefficient of earth pressure, K, equal to $1 - K_0$, is adopted to describe the difference between the lateral and vertical earth pressures (i.e. nonuniformity of earth pressure), where K_0 represents the coefficient of earth pressure at rest. Correspondingly, the lateral and vertical earth pressures can be calculated as

$$G_h = (1 - K)\gamma h \quad (1)$$

$$G_v = \gamma h \quad (2)$$

where h is the buried depth of concrete pipeline, and γ is the soil unit weight.

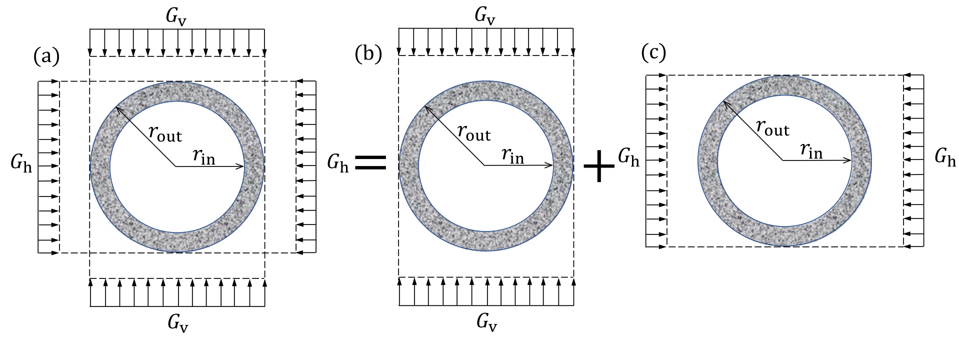

Fig. 1. Earth pressure on underground concrete pipeline: (a) both vertical and lateral pressures; (b) only vertical pressure; (c) only lateral pressure.

The superposition principle of elasticity indicates that the force state of pipeline can be decomposed into the vertical force state (Fig. 1(b)) plus the horizontal force state (Fig. 1(c)). On the surface, these two force states look different. As a matter of fact, the states can be considered identical, because it can be regarded that a circle is subjected to the force only in one direction and the stress state of circle is irrelevant to the direction where the force is acting. Hence, only the stress distribution of underground concrete pipeline in the horizontal force state needs to be calculated. Then, the stress distribution of pipeline in the vertical force state can be obtained through replacing the lateral pressure with the vertical pressure and switching the polar angles. To determine the stress distribution of pipeline in the horizontal force state, the diagram of horizontal earth pressure (Fig. 2(a)) is decomposed into two diagrams (Fig. 2(b) and (c)). Here, the compressive stress is assumed to be positive in this study. Then, as for the force diagram shown in Fig. 2(b), the boundary conditions can be written as

$$r = r_{in} : \sigma_r = 0, \tau_{r\theta} = 0 \tag{3}$$

$$r = r_{out} : \sigma_r = -\frac{\sigma_h}{2}\cos 2\theta, \tau_{r\theta} = \frac{\sigma_h}{2}\sin 2\theta \tag{4}$$

where r and θ are the polar coordinates; r_{out} and r_{in} denote the outer and inner radii of pipeline, respectively; and σ_r and $\tau_{r\theta}$ represent the radial and shear stresses, respectively.

From the boundary conditions, it can be known that the stresses in the pipeline should be a function of radial distance, $f(r)$, times $\cos 2\theta$. Therefore, the stress function, U, can be assumed as

$$U = f(r)\cos 2\theta \tag{5}$$

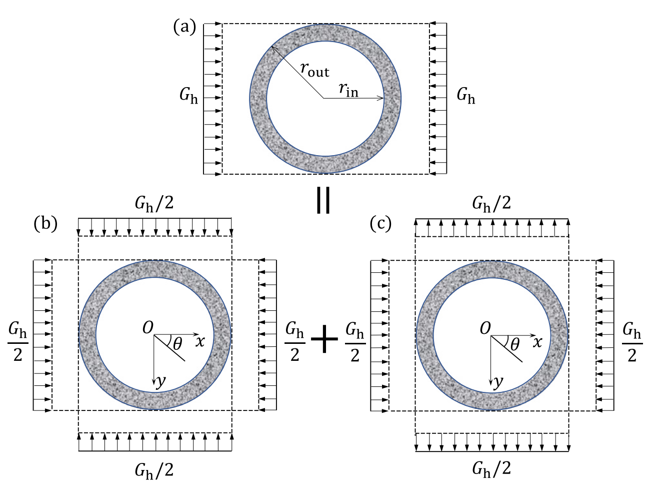

Fig. 2. Decomposition of lateral earth pressure on underground concrete pipeline.

This stress function satisfies the biharmonic function in the polar coordinate system, which is written as

$$\left(\frac{\partial^2}{\partial r^2} + \frac{1}{r}\frac{\partial}{\partial r} + \frac{1}{r^2}\frac{\partial^2}{\partial \theta^2}\right)^2 U = 0 \tag{6}$$

Substituting Eq. (5) into Eq. (6) gives

$$\left[\frac{\partial^4 f(r)}{\partial r^4} + \frac{2}{r}\frac{\partial^3 f(r)}{\partial r^3} - \frac{9}{r^2}\frac{\partial^2 f(r)}{\partial r^2} + \frac{9}{r^3}\frac{\partial f(r)}{\partial r}\right]\cos 2\theta = 0 \tag{7}$$

Solving the above equation yields the stress function as

$$U = \left(Ar^4 + Br^2 + C + \frac{D}{r^2}\right)\cos 2\theta \tag{8}$$

where A, B, C and D are the parameters for expressing the stress function, which will be determined in the following.

The stress components can be calculated based on the theory of elasticity, respectively, as

$$\sigma_r = -\left(2B + \frac{4C}{r^2} + \frac{6D}{r^4}\right)\cos 2\theta \tag{9}$$

$$\sigma_\theta = -\left(12Ar^2 + 2B + \frac{6D}{r^4}\right)\cos 2\theta \tag{10}$$

$$\tau_{r\theta} = \left(6Ar^2 + 2B - \frac{2C}{r^2} - \frac{6D}{r^4}\right)\sin 2\theta \tag{11}$$

where σ_θ is the circumferential stress.

Substituting all stress components (i.e. Eqs. (9)–(11)) into the boundary conditions (i.e. Eqs. (3) and (4)), the parameters, A, B, C and D can be determined as follows

$$C = \frac{G_h}{2}\frac{r_{in}^4 r_{out}^{10} - r_{in}^{10} r_{out}^4}{-r_{in}^2 r_{out}^{10} + 4r_{in}^4 r_{out}^8 - 6r_{in}^6 r_{out}^6 + 4r_{in}^8 r_{out}^4 - r_{in}^{10} r_{out}^2} \tag{12}$$

$$D = \frac{G_h r_{in}^4 r_{out}^8 + 8C\left(r_{in}^2 r_{out}^4 - r_{in}^4 r_{out}^2\right)}{12\left(r_{in}^4 - r_{out}^4\right)} \tag{13}$$

$$B = -\frac{2C}{r_{in}^2} - \frac{3D}{r_{in}^4} \tag{14}$$

$$A = \frac{1}{3r_{in}^2}\left(\frac{C}{r_{in}^2} + \frac{3D}{r_{in}^4} - B\right) \tag{15}$$

Then, the stress components can be specifically obtained through substituting the above four equations into Eqs. (9)–(11).

As for the force diagram shown in Fig. 2(c), it can be easily found that it is a classical axisymmetric problem in the elasticity. Hence, the radial and circumferential stresses can be simply determined based on the theory of elasticity as

$$\sigma_r = \frac{E}{r^2} + 2F \tag{16}$$

$$\sigma_\theta = -\frac{E}{r^2} + 2F \tag{17}$$

$$\tau_{r\theta} = 0 \tag{18}$$

where E and F are the parameters for expressing the stress components.

The corresponding boundary conditions can be written as

$$r = r_{\text{in}}, r = r_{\text{out}} : \sigma_r = -\frac{G_{\text{h}}}{2} \tag{19}$$

$$r = r_{\text{in}}, r = r_{\text{out}} : \tau_{r\theta} = 0 \tag{20}$$

Substituting Eqs. (16) and (17) into Eqs. (19) and (20), the stress components can be determined as

$$\sigma_r = -\frac{G_{\text{h}}}{2}\left(-\frac{r_{\text{in}}^2}{r^2} + 1\right) \tag{21}$$

$$\sigma_\theta = -\frac{G_{\text{h}}}{2}\left(\frac{r_{\text{in}}^2}{r^2} + 1\right) \tag{22}$$

$$\tau_{r\theta} = 0 \tag{23}$$

Combining Eqs. (9)–(11) and Eqs. (21)–(23), with the substitution of Eqs. (12)–(15), the stress distribution of underground concrete pipeline only subjected to lateral earth pressure can be calculated as

$$\sigma_r = -\left(2B + \frac{4C}{r^2} + \frac{6D}{r^4}\right)\cos 2\theta - \frac{G_{\text{h}}}{2}\left(-\frac{r_{\text{in}}^2}{r^2} + 1\right) \tag{24}$$

$$\sigma_\theta = \left(12Ar^2 + 2B + \frac{6D}{r^4}\right)\cos 2\theta - \frac{G_{\text{h}}}{2}\left(\frac{r_{\text{in}}^2}{r^2} + 1\right) \tag{25}$$

$$\tau_{r\theta} = \left(6Ar^2 + 2B - \frac{2C}{r^2} - \frac{6D}{r^4}\right)\sin 2\theta \tag{26}$$

As stated above, the stress distribution of underground concrete pipeline only subjected to vertical earth pressure can then be determined by replacing G_{h} with G_{v} and θ with $\theta - \pi/2$ in Eqs. (24)–(26). Combining the two kinds of stress distributions, the stress distribution of underground concrete pipeline subjected to nonuniformly distributed earth pressures can be finally determined.

2.2. Effect of stress distribution on chloride diffusion coefficient

It can be easily found from Eq. (25) that the circumferential stress can show different states, i.e. compressive or tensile state, on different cross sections because of different corresponding values of angle θ. This is an important aspect different from the state of circumferential stress in the underground concrete pipeline subjected to uniformly distributed earth pressure, since its circumferential stress is always compressive. When the circumferential stress is the tensile stress, it greatly affects the void ratio of concrete as well as the generation and development of initial cracks, which further significantly affects the chloride diffusion rate in the concrete pipeline. To describe the chloride diffusion process in the underground concrete pipeline subjected to nonuniformly distributed earth pressures, the empirical relations of diffusion coefficient for different stress states obtained by Li [16] is adopted, which are listed as follows

$$D_\sigma^t = D_0\left(1 + Q_{t1}\overline{\sigma} + Q_{t2}\overline{\sigma}^2\right)(\text{tensile state}) \tag{27}$$

$$D_\sigma^c = D_0\left(1 + Q_{c1}\overline{\sigma} + Q_{c2}\overline{\sigma}^2\right)(\text{compressive state}) \tag{28}$$

where $\overline{\sigma}$ denotes the stress level, equal to $\overline{\sigma} = \sigma/f_t$ for the tensile state and $\overline{\sigma} = \sigma/f_c$ for the compressive state, respectively; σ is the acting stress; f_t and f_c are the tensile and compressive strengths of concrete; Q_{t1} and Q_{t2} are the fitting coefficients for the tensile state and equal to 0.4184 and −0.1239, respectively; Q_{c1} and Q_{c2} are the fitting coefficients for the compressive state, which equal 0.0968 and −0.5507, respectively; and D_0 represents the chloride diffusion coefficient in the uncracked concrete, equal to [17]

$$D_0 = 10\exp\left[-3.9(w/c)^2 + 7.2(w/c) - 14.0\right] \tag{29}$$

where w/c denotes the water-cement ratio.

The reason for adopting the empirical relationship proposed by Li [16] to describe the chloride diffusion in the underground concrete pipeline subjected to nonuniformly distributed earth pressures is that compared with other empirical relationships, this relationship considers the tensile and compressive strengths of concrete and thus it can provide more practical guiding significance.

2.3. Solution of diffusion equation

As mentioned above, the stress in the circumferential direction varies with the angle, θ, as the underground concrete pipeline is subjected to nonuniformly distributed earth pressure and can become either compressive or tensile stress, which results in the nonuniform chloride diffusion along the radial direction. In another word, with different values of angle, θ, the diffusion of chloride ions is different in each radial direction. Therefore, the diffusion in the radial direction should be considered with each individual value of angle, θ, based on the directions of stress extreme values obtained from the solution of stress distribution. Then, the location where the chloride ion concentration firstly reaches the critical concentration resulting in the steel corrosion can be determined. Additionally, the service life of underground pipeline under the nonuniformly distributed earth pressures in the diffusion period can be estimated. To achieve these aims, the chloride diffusion in the radial direction with each individual angle, θ, can be modelled based on the diffusion in the compound media in the Cartesian coordinate system.

As shown in Fig. 3, the coordinate system is built by setting the center of pipeline as the origin and the radial direction as the x axis. The concrete cover is divided into m layers along the x axis. The coordinate of inner surface is denoted as x_1 and the coordinate of outer surface is set as x_m. Because each concrete layer is subjected to different stress levels, the diffusion coefficients of each layer are different, which are denoted as D_i $(i = 1, 2, 3, \cdots, m)$. When the pipeline is just buried in the chlorinated soil, the chloride ion concentration of each inner concrete layer equals zero. The concentration at the outer surface equals the equilibrium chloride ion

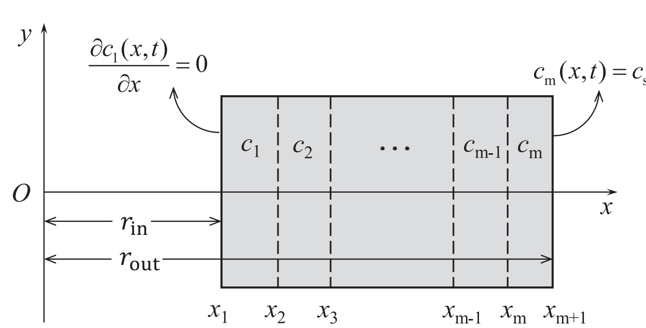

Fig. 3. Diffusion in compound media in Cartesian coordinate system.

concentration of surrounding soil, c_s, since it is completely exposed to the outer chlorinated environment. As time goes on, the chloride ions at the outer surface diffuse inwards. In comparison, the chloride ions at the inner surface do not diffuse further, because it is isolated from the outer chlorinated environment.

The governing equation of chloride diffusion can be given, according to the Fick's second law, as

$$\frac{\partial c_i(x,t)}{\partial t} = D_i \frac{\partial^2 c_i}{\partial x^2}, x_i < x < x_{i+1}, i = 1, 2, ..., m \tag{30}$$

where t is the time; and c_i represents the chloride ion concentration of the ith concrete layer.

The corresponding boundary and initial conditions can be written as

$$\begin{cases} \frac{\partial c_i(x,t)}{\partial t} = 0, x = x_1 \\ c_m(x,t) = c_s, x = x_{m+1} \end{cases} \tag{31}$$

$$c_i(x,0) = 0, x_i < x < x_{i+1} \tag{32}$$

The continuity condition for the influx and flux of chloride ions should be satisfied at the interface between the concrete layers, which can be expressed as

$$\begin{cases} D_i \frac{\partial c_i(x,t)}{\partial t} = D_{i+1} \frac{\partial c_{i+1}(x,t)}{\partial t} \\ c_i(x,t) = c_{i+1}(x,t) \end{cases}, x = x_{i+1}, i = 1, 2, \cdots, m-1 \tag{33}$$

With the aid of these boundary and initial conditions, the theory of partial differential equation indicates that the mathematical problem for solving Eq. (30) can be separated into a homogeneous unstable state diffusion problem along with two nonhomogeneous stable state diffusion problems. Therefore, the solution of Eq. (30) is the sum of the solutions of these three problems. The specific derivation processes of the solutions of these three problems have been given by Wang et al [18] in detail. Here, only the final solution of Eq. (30) is given as

$$c_i(x,t) = c_s \vartheta_i(x,t) + \omega_i(x,t), i = 1, 2, \cdots, m \tag{34}$$

where

$$\vartheta_i(x) = 1 \tag{35}$$

$$\omega_i(x,t) = \sum_{n=1}^{\infty} e^{-\beta_n^2 t} \frac{1}{N_n} \chi_{in}(\beta_n, x) \sum_{j=1}^{m} \int_{x_j}^{x_{j+1}} -c_s x \chi_{jn}(x) dx \tag{36}$$

In Eq. (36), β_n are the eigenvalues when the determinant of coefficient for the governing equation equals zero; N_n is a parameter for simplifying the equation expression; and χ_{in} is the eigenfunction. The expressions of N_n and χ_{in} are written as

$$N_n = \sum_{i=1}^{m} \int_{x_i}^{x_{i+1}} x \chi_{in}^2(\beta_n, x) dx \tag{37}$$

$$\chi_{in}(x) = A_{in} \sin\left(\frac{\beta_n}{\sqrt{D_i}} x\right) + B_{in} \cos\left(\frac{\beta_n}{\sqrt{D_i}} x\right) \tag{38}$$

To show how to specifically solve the problem, the following derives the solution of characteristic equation for four-layer compound media. Based on the boundary and continuity conditions, the corresponding characteristic equation should satisfy the following homogenous linear equations as

$$\begin{bmatrix} M_{11} & M_{12} \\ M_{21} & M_{22} \end{bmatrix} \begin{pmatrix} L_{11} \\ L_{21} \end{pmatrix} = \begin{pmatrix} 0 \\ 0 \end{pmatrix} \tag{39}$$

where M_{11}, M_{12}, M_{21} and M_{22} are the block matrices and their expressions are written as

$$M_{11} = \begin{bmatrix} \cos(\eta_1) & -\sin(\eta_1) & 0 & 0 \\ P_1 \cos\left(\frac{\eta_1 x_2}{x_1}\right) & P_1 \sin\left(\frac{\eta_1 x_2}{x_1}\right) & -\cos(\eta_2) & \sin(\eta_2) \\ \sin\left(\frac{\eta_1 x_2}{x_1}\right) & \cos\left(\frac{\eta_1 x_2}{x_1}\right) & -\sin(\eta_2) & -\cos(\eta_2) \\ 0 & 0 & P_2 \cos\left(\frac{\eta_2 x_3}{x_2}\right) & -P_2 \sin\left(\frac{\eta_2 x_3}{x_2}\right) \end{bmatrix} \tag{40}$$

$$M_{12} = \begin{bmatrix} 0 & 0 & 0 & 0 \\ 0 & 0 & 0 & 0 \\ 0 & 0 & 0 & 0 \\ -\cos(\eta_3) & -\sin(\eta_3) & 0 & 0 \end{bmatrix} \tag{41}$$

$$M_{21} = \begin{bmatrix} 0 & 0 & \sin\left(\frac{\eta_2 x_3}{x_2}\right) & \cos\left(\frac{\eta_2 x_3}{x_2}\right) \\ 0 & 0 & 0 & 0 \\ 0 & 0 & 0 & 0 \\ 0 & 0 & 0 & 0 \end{bmatrix} \tag{42}$$

$$M_{22} = \begin{bmatrix} -\sin(\eta_3) & -\cos(\eta_3) & 0 & 0 \\ P_3 \cos\left(\frac{\eta_3 x_4}{x_3}\right) & -P_3 \sin\left(\frac{\eta_3 x_4}{x_3}\right) & -\cos(\eta_4) & \sin(\eta_4) \\ \sin\left(\frac{\eta_3 x_4}{x_3}\right) & \cos\left(\frac{\eta_3 x_4}{x_3}\right) & -\sin(\eta_4) & -\cos(\eta_4) \\ 0 & 0 & \sin\left(\frac{\eta_4 x_5}{x_4}\right) & \cos\left(\frac{\eta_4 x_5}{x_4}\right) \end{bmatrix} \tag{43}$$

$$L_{11} = \begin{pmatrix} 1 \\ B_{1n} \\ A_{2n} \\ B_{2n} \end{pmatrix}, L_{21} = \begin{pmatrix} A_{3n} \\ B_{3n} \\ A_{4n} \\ B_{4n} \end{pmatrix} \tag{44}$$

where

$$\begin{cases} \eta_1 = x_1 \frac{\beta_n}{\sqrt{D_1}} \\ \eta_2 = x_2 \frac{\beta_n}{\sqrt{D_2}} \\ \eta_3 = x_3 \frac{\beta_n}{\sqrt{D_3}} \\ \eta_4 = x_4 \frac{\beta_n}{\sqrt{D_4}} \end{cases} \tag{45}$$

$$\begin{cases} P_1 = \sqrt{\frac{D_1}{D_2}} \\ P_2 = \sqrt{\frac{D_2}{D_3}} \\ P_3 = \sqrt{\frac{D_3}{D_4}} \end{cases} \tag{46}$$

where the eigenvalues, β_n $(n = 1, 2, 3, 4)$, can be determined by making the determinant of coefficient of Eq. (39) equal to zero. Then, the parameters A_{in} and B_{in} $(i = 1, 2, 3, 4)$ can be calculated through solving Eq. (39) as below

$$B_{1n} = \frac{\cos(\eta_1)}{\sin(\eta_1)} \tag{47}$$

$$A_{2n} = \frac{P_1\left[\cos\left(\frac{\eta_1 x_2}{x_1}\right) + F_{1n} \sin\left(\frac{\eta_1 x_2}{x_1}\right)\right] + F_{2n} \sin(\eta_2)}{\cos(\eta_2)} \tag{48}$$

$$B_{2n} = [\cos(\eta_2) + P_1 \sin(\eta_2) F_{1n}] \sin\left(\frac{\eta_1 x_2}{x_1}\right) + [F_{1n} \cos(\eta_2) - P_1 \sin(\eta_2)] \cos\left(\frac{\eta_1 x_2}{x_1}\right) \tag{49}$$

$$A_{3n} = \frac{P_2\left[E_{2n}\cos\left(\frac{\eta_2 x_3}{x_2}\right) - F_{2n}\sin\left(\frac{\eta_2 x_3}{x_2}\right)\right] + F_{3n}\sin(\eta_3)}{\cos(\eta_3)} \tag{50}$$

$$B_{3n} = \cos(\eta_3)\left[E_{2n}\sin\left(\frac{\eta_2 x_3}{x_2}\right) + F_{2n}\cos\left(\frac{\eta_2 x_3}{x_2}\right)\right] - P_2\sin(\eta_3)\left[E_{2n}J_1\left(\frac{\eta_2 x_3}{x_2}\right) + F_{2n}Y_1\left(\frac{\eta_2 x_3}{x_2}\right)\right] \tag{51}$$

$$A_{4n} = \frac{P_3\left[E_{3n}\cos\left(\frac{\eta_3 x_4}{x_3}\right) - F_{3n}\sin\left(\frac{\eta_3 x_4}{x_3}\right)\right] + F_{4n}\sin(\eta_4)}{\cos(\eta_4)} \tag{52}$$

$$B_{4n} = \cos(\eta_4)\left[E_{3n}\sin\left(\frac{\eta_3 x_4}{x_3}\right) + F_{3n}\cos\left(\frac{\eta_3 x_4}{x_3}\right)\right] - P_3\sin(\eta_4)\left[E_{3n}\cos\left(\frac{\eta_2 x_3}{x_2}\right) + F_{3n}\sin\left(\frac{\eta_2 x_3}{x_2}\right)\right] \tag{53}$$

where J_1 and Y_1 are the first-order first kind and second kind Bessel functions; and E_{jn} $(j = 2, 3)$ and F_{kn} $(k = 1, 2, 3)$ are the parameters for the analytical solution of underground concrete pipeline subjected to uniformly distributed earth pressure and their expressions can be specifically found in the Appendix.

Combining Eqs. (34), (35) and (36)–(52), the chloride diffusion in the four-layer compound media can be determined. Here, the chloride ion threshold level is taken as the ratio of chloride ion content to cement content, because this criterion considers the cement hydration inhibiting effect as well as free chloride ions recombination. According to the summarization of critical chloride ion contents reported by Shao and Li [19], it can be known that the critical value of the ratio of chloride ion content to cement content generally varies from 0.2% to 3.08%. As a result, the pipeline service life in this period, T_D, can be determined through solving Eq. (30), with the substitution of the steel bar radial location and the critical chloride ion content.

3. Protective cover cracking caused by corrosion expansion

3.1. Basic assumptions

To estimate the service life of underground concrete pipeline under the nonuniformly distributed earth pressure in the chloride contaminated environment, the concrete pipeline is simulated as the dual compound media consisting of the corrosion products and outer productive cover, which is just shown in Fig. 4. The outer protective cover is subjected to the forces from three directions, which are the vertical earth pressure, G_v, the lateral earth pressure, G_h, and the uniformly distributed corrosion expansion pressure, P_r. The notations R_4 and R_4 denote the outer and inter radii of the mechanical model. As the circumferential tensile stress at the inner surface of outer productive cover arrives at the concrete tensile strength, the thickness of corrosion products between the concrete and steel bar can be determined from the displacement superposition of pipeline subjected to the aforementioned three kinds of pressures. Before deriving the solution of the displacement caused by each kind of pressure, four basic assumptions need to be made here, which are given in the following:

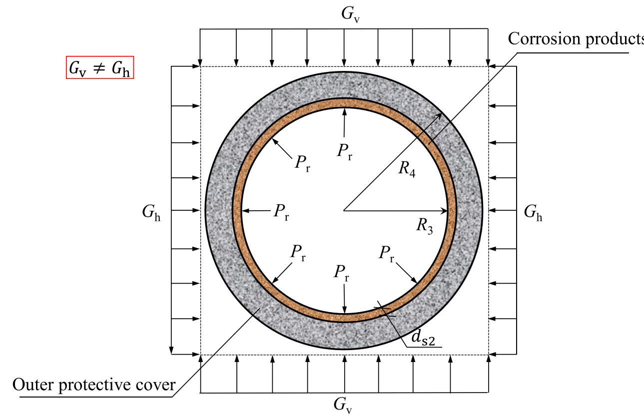

Fig. 4. Mechanical model of dual compound media composed of corrosion products and outer protective cover.

(i) The concrete material made into the outer productive cover exhibits the linear elasticity and its corresponding mechanical properties remain constant before cracking;
(ii) The concrete and steel bar are not fully contacted and there are micro voids consisting of porous zone at the concrete-steel surface. Once the steel begins to rust, the corrosion products fill in the porous zone at first;
(iii) The corrosion products around the steel bar are uniformly distributed. Thus, the corrosion expansion pressure is acting uniformly on the steel bar and the productive cover;
(iv) In fact, the cracking of concrete cover is attributed to many factors, such as shrinkage, chemical reactions, thermal changes, overloading, premature drying and the like. If all of these factors are taken into consideration, it is impossible to build the analytical model since the solution to the analytical model will become extremely complex and quite difficult to solve, let alone putting it into practice. Therefore, for sake of deriving the analytical solution, only the cracking caused by the corrosion expansion pressure and the nonuniformly distributed earth pressure are taken into account.

3.2. Mechanical analysis of protective cover

According to the above assumptions and the theory of elasticity, the circumferential strain of underground concrete pipeline only resulting from the lateral earth pressure, $\varepsilon_{\theta 1}$, can be easily obtained just through substituting the stress equations (i.e. Eqs. (24) and (25)) into the following physical equation, i.e.

$$\varepsilon_\theta = \frac{\sigma_c - \upsilon\sigma_r}{E_e} \tag{54}$$

where ε_θ is the circumferential strain; E_e is the concrete effective elastic modulus, calculated as $E_c/(1+\varphi_{cr})$; and υ is the concrete Poisson's ratio. The notations, φ_{cr}, and E_c represent the creep coefficient and elastic modulus of concrete, respectively.

The expression of $\varepsilon_{\theta 1}$ can be written after the substitution as

$$\varepsilon_{\theta 1} = \frac{1}{E_e}\left[-\left[2B + \frac{4C}{r^2} + \frac{6D}{r^4} - \upsilon\left(12Ar^2 + 2B + \frac{6D}{r^4}\right)\right]\cos 2\theta - \frac{G_h R_4^2}{2\left(R_4^2 - R_3^2\right)}\left[\left(1 - \frac{R_3^2}{r^2}\right) - \upsilon\left(\frac{R_3^2}{r^2} + 1\right)\right]\right] \tag{55}$$

Substituting the above equation into the geometric equation (i.e. $\varepsilon_\theta = \partial u_r/\partial r$ and u_r represents the radial displacement), integrating the equation and determining the integration constant based on the axisymmetric condition, the radial displacement in the underground concrete pipeline can be determined as

$$u_{r1} = \frac{1}{E_e}\left[-\left[2Br - \frac{4C}{r} - \frac{2D}{r^3} - v\left(4Ar^3 + 2Br - \frac{2D}{r^3}\right)\right]\cos 2\theta - \frac{G_h R_4^2}{2\left(R_4^2 - R_3^2\right)}\left[\left(\frac{R_3^2}{r} + 1\right) + v\left(1 - \frac{R_3^2}{r}\right)\right]\right] \tag{56}$$

As for the situation that the underground concrete pipeline only subjected to vertical earth pressure, the displacement can be calculated just through replacing the lateral earth pressure, G_h, with the vertical earth pressure, G_v, as well as the polar angle, θ, with the polar angle, $\theta - \frac{\pi}{2}$. The superposition of displacement solutions caused by two-direction earth pressures yields the final displacement solution of underground concrete pipeline subjected to nonuniformly distributed earth pressures.

The circumferential stress in the underground concrete pipeline arising from the corrosion expansion pressure, $\sigma_{\theta 3}$, can be easily calculated on the basis of the theory of elasticity via assuming the corrosion expansion pressure as P_r, in the following

$$\sigma_{\theta 3} = \frac{P_r R_3^2}{R_4^2 - R_3^2}\left(1 + \frac{R_4^2}{r^2}\right) \tag{57}$$

The corresponding displacement in underground concrete pipeline can be calculated as

$$u_{r3} = \frac{P_r R_3^2}{E_e r\left(R_4^2 - R_3^2\right)}\left[\left(r^2 + r_4^2\right) + v_c\left(R_4^2 - r^2\right)\right] \tag{58}$$

Therefore, the superposition of stress solutions resulting from the three-kind pressures yields the stress distribution in the underground concrete pipeline subjected to nonuniformly distributed earth pressures. Making the radial distance equal to the inner radius (i.e. $r = R_3$), the circumferential stress at the inner surface of outer protective cover at each angle, θ, can be determined and it is easily found that the circumferential stress changes with the change in the value of angle θ. When the angle θ reaches a certain value, θ_m, the circumferential stress can arrive at the maximum value, $\sigma_{\theta\max}$. As the maximum value of circumferential stress increases to the concrete tensile strength, f_t, (i.e. $\sigma_{\theta\max} = f_t$), the corrosion expansion pressure, P_r, can determined as

$$P_r = \left(f_t - \sigma_{\theta m1} - \sigma_{\theta m2}\right)\frac{R_4^2 - R_3^2}{R_3^2 + R_4^2} \tag{59}$$

where $\sigma_{\theta m1}$ and $\sigma_{\theta m2}$ are the circumferential stresses at the inner surface of outer protective cover resulting from lateral and vertical earth pressures, respectively, as the angle θ reaches the certain value, θ_m.

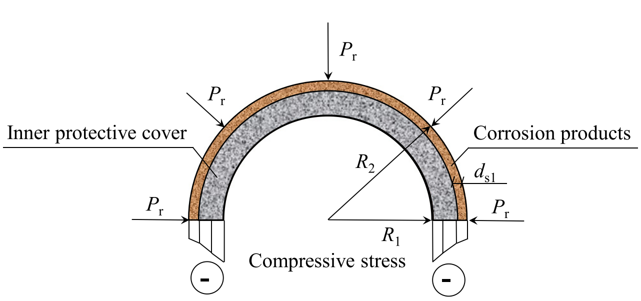

Fig. 5. Mechanical model of inner protective cover and corrosion products.

Substituting the corrosion expansion pressure, P_r, (i.e. Eq. (59)) and $r = R_3$ into Eq. (58) and summing the three displacement solutions, the radial displacement of protective cover is able to be determined. Since the thickness of corrosion products, d_{s2}, equals the radial displacement of protective cover, the thickness of corrosion products, d_{s2}, can be determined as well.

Due to the corrosion expansion pressure, the inner protective cover is compressed towards the center of pipeline and the corresponding radial displacement is negative, which is just shown in Fig. 5. In the figure, R_2 and R_1 denote the outer and inner radii of inner protective cover. The corrosion products of steel bar fill in the porous zone arising from this radial displacement after the steel bar rusts. Therefore, the thickness of corrosion products around steel bar, d_{s1}, equals the negative radial displacement of inner protective cover, which is able to be easily calculated on the basis of the theory of elasticity as

$$d_{s1} = \frac{P_r R_2\left[\left(R_2^2 + R_1^2\right) + v\left(R_1^2 - R_2^2\right)\right]}{E_e\left(R_2^2 - R_1^2\right)} \tag{60}$$

3.3. Mass of corrosion products and pipeline service life

The total mass of corrosion products is composed of three parts, which are the mass of corrosion products filling in the porous zone at the concrete-steel interface, m_e, the mass of corrosion products yielding expansion pressures, m_p, and the mass of corrosion products filling in the steel bar loss because of corrosion, m_l. The expressions of three parts can be written as

$$m_e = 2\rho_c\pi\left[R_2 d_0 + (R_2 + d_0 + d_s)d_0\right] \tag{61}$$

$$m_p = 2\rho_c\pi\left[R_3 d_{s2} + (R_2 - d_{s1})d_{s1}\right] \tag{62}$$

$$m_l = \rho_c\frac{m_{st}}{\rho_{st}} = \rho_c\frac{m_T\omega}{\rho_{st}} \tag{63}$$

where ρ_c denotes the density of corrosion products; d_0 is the thickness of porous zone around steel-concrete interface; ρ_{st} is the steel bar density; d_s represents the initial steel bar diameter; m_{st} is the loss weight of steel bar; and ω is the ion mass proportion in corrosion products, the value of which varies from 0.523 to 0.622 [20].

Summing the three parts up yields the total mass of corrosion products, m_T, as

$$m_T = \frac{2\pi\rho_{st}\rho_r}{\rho_{st} - \rho_r\omega}\left[R_2 d_0 + (R_2 + d_0 + d_s)d_0 + R_3 d_{s2} + (R_2 - d_{s1})d_{s1}\right] \tag{64}$$

As the corrosion layer thickness increases, the diffusion distance of ions increases and correspondingly the production rate of corrosion decreases [20]. Therefore, the corrosion productivity, J_{cor}, can be determined, since it is inversely proportional to the total weight of corrosion products, as follows

$$J_{cor} = \frac{dm_T(t)}{dt} = \frac{k_p}{m_T(t)} \tag{65}$$

where k_p is the production rate and depends on the corrosion rate of steel bar, able to be determined using the corrosion rate as [21]

$$k_p = 0.098 - \frac{\pi i_{cor} d_s}{1.08\omega} \tag{66}$$

where i_{cor} is the electric current density of corrosion. Note that the units of production rate of corrosion products, k_p, and corrosion electric current density, i_{cor}, are $\text{kg}/(\text{m}^2 \cdot a)$ and $\mu\text{A/cm}^2$, respectively.

When the total mass of corrosion products is determined (i.e. Eq. (64)), the pipeline service life during corrosion can be determined via solving Eq. (65) as

$$T_{cor} = \frac{\omega m_T^2}{0.196\pi d_s i_{cor}} \tag{67}$$

As the pipeline service life during corrosion is determined, the whole service life of pipeline in the chlorinated soil can be finally determined by summing up the service life of diffusion period and the service life of corrosion period.

4. Finite element modeling for verification

To examine the validity of proposed solution for predicting the chloride diffusion in the underground concrete pipeline subjected to nonuniformly distributed earth pressures, a two-dimensional finite-element model is built with ABAQUS. The chloride diffusion is simulated by means of the heat transfer module. As shown in Fig. 6, the x coordinates of outer and inner surfaces of protective cover model are 0.42 m and 0.3 m, respectively. The model is divided equally into four layers and the diffusion coefficients of each layer from the inside out are $D_1 = 2.0 \times 10^{-12}$ m^2/s, $D_2 = 3.0 \times 10^{-12}$ m^2/s, $D_3 = 4.0 \times 10^{-12}$ m^2/s, and $D_4 = 5.0 \times 10^{-12}$ m^2/s, respectively. Note that no chloride diffusion occurs at the inner surface of protective cover and the constant chloride ion concentration of protective cover, c_s, is 0.346% of the concrete weight [22]. The sweeping method and the linear heat transfer quadrilateral element are employed to divide the finite-element model into 64 elements. The diffusion coefficient of uncracked concrete, D_0, equals 0.76×10^{-12} m^2/s [23].

Fig. 7 illustrates the distribution contour of chloride ion concentration after different exposure periods. It can be found that the chloride diffusion in the concrete cover can be effectively simulated through the established finite element model. At the same x coordinate, the chloride ion concentration remains constant along the y axis. The chloride ion concentration shows a decrease trend from the outer surface to the inner surface. The chloride ion concentration arrives at the maximum value at the outer surface, equaling the chloride ion concentration of surrounding soil, while at the inner surface the chloride ion concentration arrives at the minimum value. This is because the chloride ions diffuse from the outer surface to the inter surface and the chloride ions at the inner surface do not diffuse further.

Fig. 8 shows the comparison of chloride ion concentration after different exposure periods along the data path selected in Fig. 7(b) between the proposed analytical analysis and the finite element simulation. The chloride ion concentration at the radial distance, r, is normalized with that at the outer surface of concrete cover. The radial distance, r, is normalized with the relative radius, $x' = (x - a)/(b - a)$. It can be observed from the figure that the chloride ion concentration after different exposure periods predicted by analytical solution show good agreements with the numerical results from finite element simulation, which strongly demonstrates that the proposed analytical method can appropriately estimate the diffusion of chloride ions in underground concrete pipelines subjected to nonuniformly distributed earth pressures. In addition, the verification of present diffusion model provides reliable results for the subsequent analysis of service life in the corrosion period.

5. Case analysis and parametric study

5.1. Pipeline service life of diffusion period

To explore the effects of nonuniformly distributed earth pressures and the thickness of concrete protective cover on the pipeline service life in the period of diffusion, the concrete pipeline with unit length is taken as a case for analysis. In the analysis, the pipeline inner radius equals 0.3 m. The initial thickness of protective cover is 30 mm. The unit weight of overlaying soil of concrete pipeline is 18 kN/m^3 and the initial nonhomogeneous coefficient of earth pressure, K, equals 0.5. The critical chloride ion concentration, c_{cr}, is 0.237% of concrete weight and the constant chloride ion concentration, c_s, is 0.346% of concrete weight. The concrete elastic modulus, E_c, and Poisson's ratio, υ, equal 27 GPa and 0.18, respectively. The creep coefficient of concrete is taken as 2.0. With these parameters, the evaluation of service life in the diffusion period are conducted.

Fig. 9 shows the distributions of circumferential stress of concrete protective cover when the vertical and lateral earth pressures are taken as 180 kPa and 90 kPa, respectively. The stress distributions of concrete protective cover are illustrated in Fig. 10(a) and (b) as well. From the figures, it can be found that the circumferential stress varies periodically with the variation of angle, θ, and the

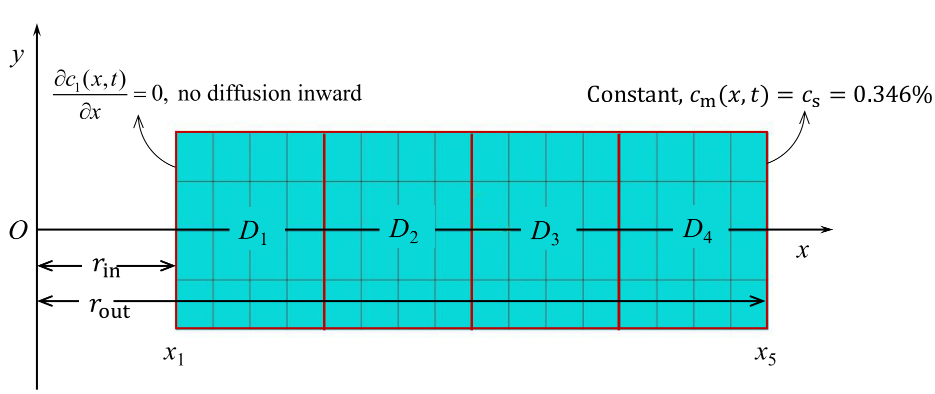

Fig. 6. Two-dimensional finite element model for four-layer compound media in Cartesian coordinate system.

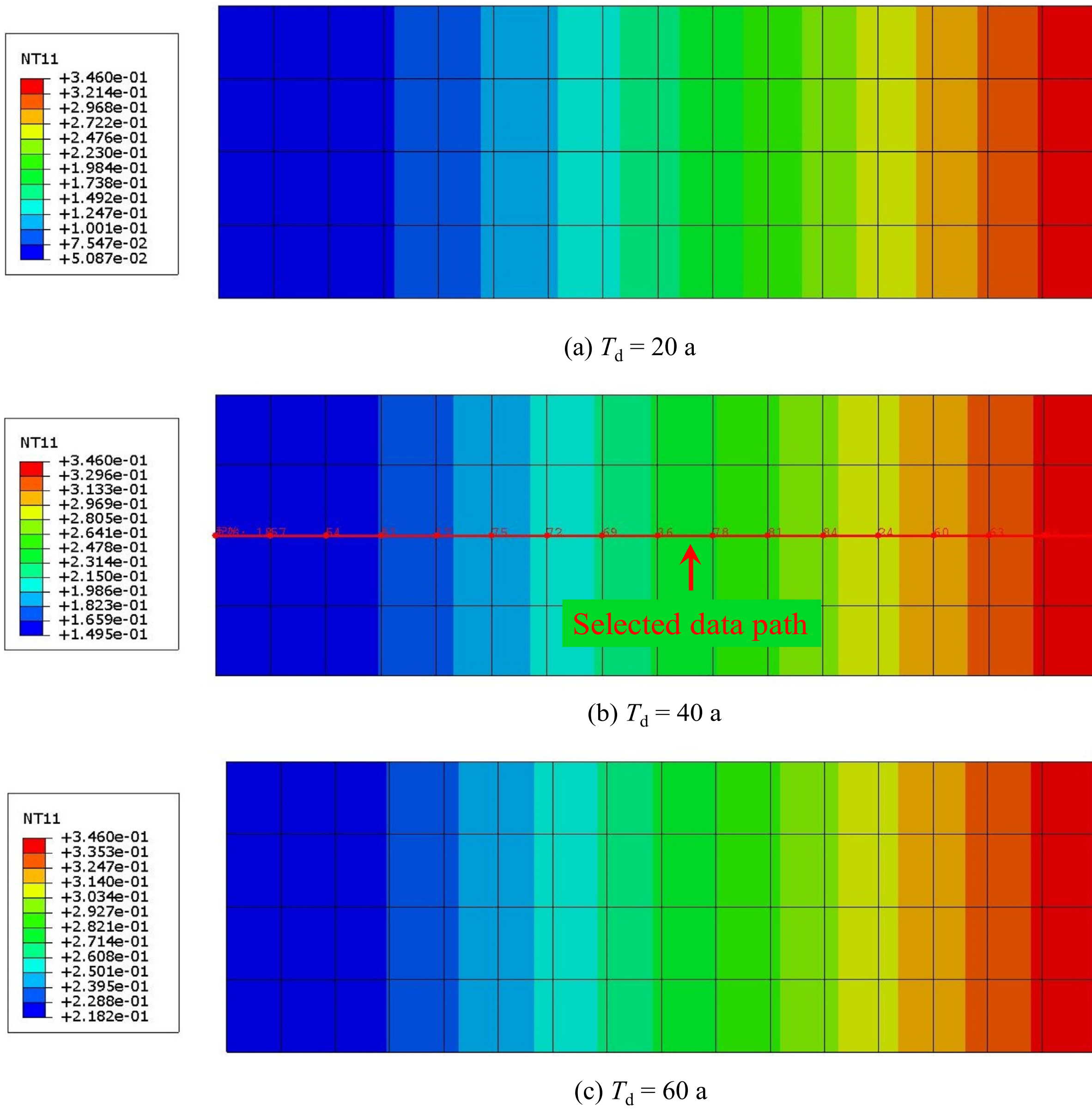

Fig. 7. Distribution contours of chloride ion concentration after different exposure periods: (a) $T_d = 20a$; (b) $T_d = 40a$; (c) $T_d = 60a$.

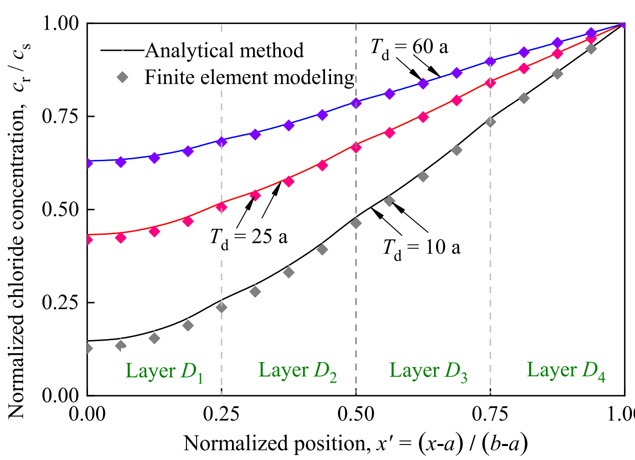

Fig. 8. Comparison of chloride ion concentration between analytical analysis and finite element modeling.

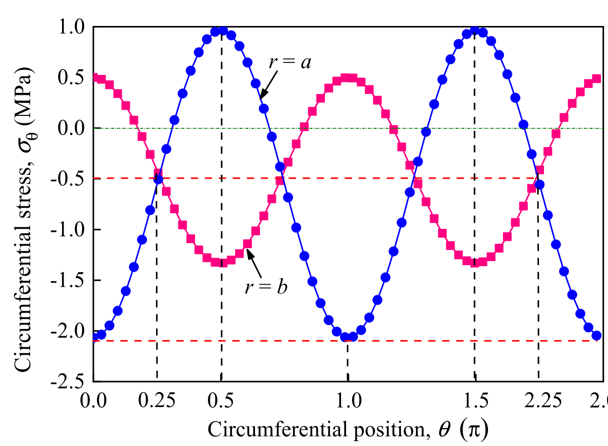

Fig. 9. Circumferential stress at inner and outer surfaces of concrete cover with different circumferential positions.

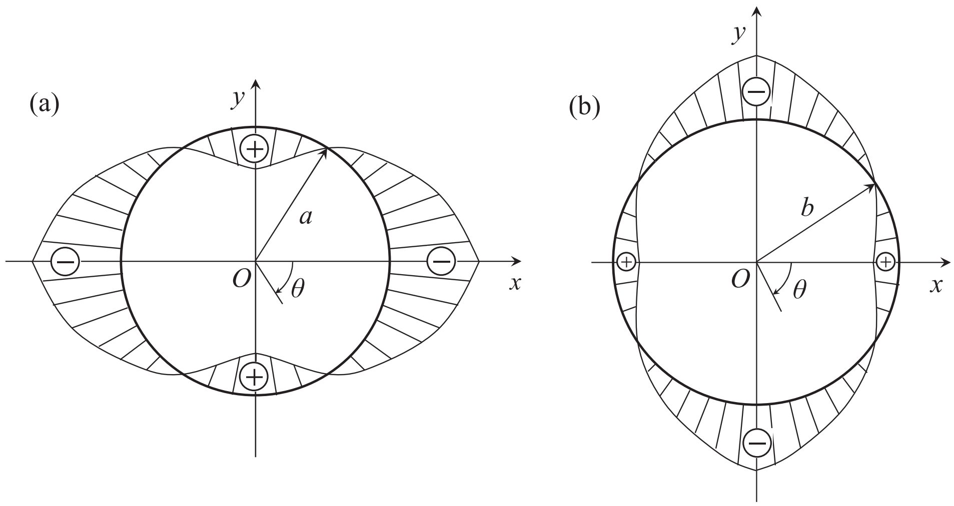

Fig. 10. Schematic of Circumferential stress distributions of concrete cover: (a) inner surface; (b) outer surface.

length of monotony interval is $\pi/2$. For the inner surface of concrete cover, when the angle, θ, equals $\pi/2$ and $3\pi/2$, the circumferential stress is the tensile stress and reaches the maximum value; when the angle, θ, is equal to 0 and π, the circumferential stress belongs to the compressive stress and arrives at the maximum value. On the contrary, the circumferential stress at the outer surface of concrete cover shows the opposite variation trend. When the angle, θ, equal $\pi/2$ and $3\pi/2$, the circumferential stress is the compressive stress and arrives at the maximum value, while as the angle, θ, equal 0 and π, the circumferential stress is the tensile stress and reaches the maximum value. It should also be noticed that when the angle, θ, equal $\pi/4$, $3\pi/4$, $5\pi/4$ and $7\pi/4$, the circumferential stresses at the inner and outer surfaces of concrete cover almost equal each other and both of them are the compressive stress. For both inner and outer surfaces of concrete cover, the range of angle, θ, that leads the circumferential stress to being the compressive stress is larger than the range leading the circumferential stress to being the tensile stress. Moreover, the maximum value of compressive stress is larger than the maximum value of tensile stress. These two phenomena indicate that the circumferential stress of underground concrete pipeline show different states, i.e. tensile or compressive stress, when the pipeline is subjected to nonuniformly distributed earth pressures. However, the compressive state takes the dominant place between the two states.

As mentioned above, the length of monotony interval of circumferential stresses is $\pi/2$, therefore Fig. 11 shows the variation of circumferential stresses along with the radial direction with different values of angle, θ, within the range from 0 to $\pi/2$. It can be observed that for each angle, θ, the circumferential stress varies with the different positions in the radial direction. The amplitude of variation first decreases and then increases as the angle, θ, increases from 0 to $\pi/2$. When the angle θ equals $\pi/4$, the circumferential stress almost remains constant along with the radial direction, which illustrates that in the concrete protective cover, there is a radial line, on which the compressive stress is nearly equal. Simultaneously, it is worth noting that when the relative radius is equal to 0.54, the circumferential stresses of each angle, θ, are the compressive stress and equal each other. This illustrates that in the concrete protective cover, there is a circumferential line, on which the compressive stress keeps the same. Moreover, it can be found that for the zone where there are both compressive and tensile stresses, the zone for compressive stress is always larger than the zone for tensile stress and the maximum value of compressive stress is larger than the maximum value of tensile stress. This demonstrates again that the compressive stress takes the dominant place as the underground concrete pipeline is subjected to nonuniformly distributed earth pressures.

Fig. 12 describes the variation of chloride diffusion coefficient along the radial direction for different circumferential positions.

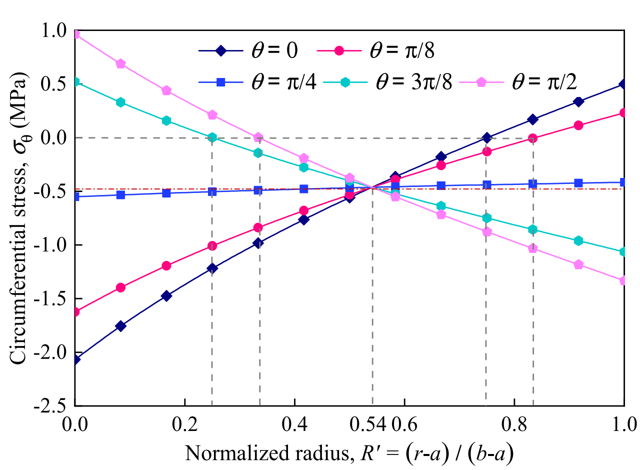

Fig. 11. Circumferential stress along with radial direction for different circumferential positions.

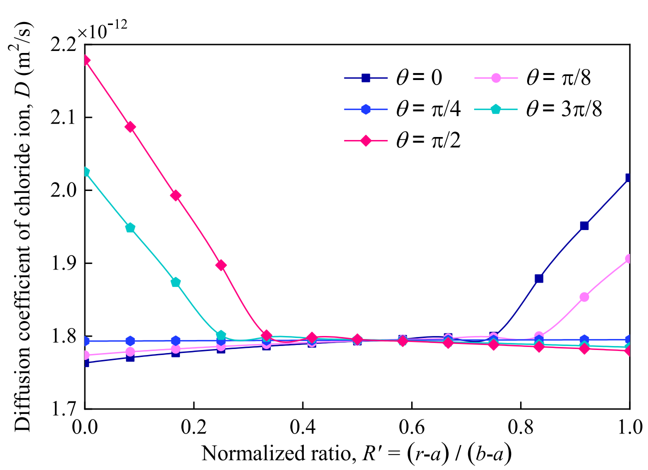

Fig. 12. Chloride diffusion coefficient along with radial direction for different circumferential positions.

It can be found that the chloride diffusion coefficient along the radial direction for each angle, θ, shows the similar variation trend as the variation of stress in Fig. 11. The chloride diffusion coefficient in the tensile zone for each angle, θ, is obviously larger than the diffusion coefficient in the zone without stress, while the chloride diffusion coefficient in the compressive zone is smaller than the diffusion coefficient in the zone without stress. It is worth noting that the variation range in the tensile zone is apparently larger than the variation in the compressive zone. When the angle θ equals $\pi/2$ and the relative radius equals 0, the variation range in the tensile zone reaches the maximum value, which is equal to 0.37×10^{-12} m^2/s (from 1.80×10^{-12} m^2/s to 2.17×10^{12} m^2/s). In comparison, when the angle θ equals 0 and the relative radius equals 0, the variation range in the compressive zone arrives at the maximum value, which is equal to 0.04×10^{-12} m^2/s (from 1.80×10^{-12} m^2/s to 1.76×10^{12} m^2/s) and is much smaller than the value of variation range in the tensile zone. This is because at a relatively low stress level, the void ratio of concrete decreases as the compressive stress increases, which consequently leads to the decrease in the chloride diffusion coefficient. On the contrary, the void ratio of concrete increases as the tensile stress increases in the tensile zone. Consequently, some original micro cracks develop further and some new micro cracks is generated. Correspondingly, some macro cracks will be generated, which will significantly increase the chloride diffusion rate in the underground concrete pipeline.

Fig. 13 illustrates the variation of chloride ion concentration at the steel bar with different thicknesses of concrete protective cover, nonhomogeneous coefficients of earth pressure and earth pressures at different circumferential locations. It should be pointed out that the exposure period of underground concrete pipeline in the chlorinated soil is assumed as 20 years. From the figure, it can be seen that the chloride ion concentration decreases as the angle, θ, increases, when the earth pressure and the thickness of concrete protective cover are constant. Therefore, at the circumferential position $\theta = 0$, the chloride ion concentration at the steel bar will reach the critical chloride ion concentration of steel corrosion at first. In another word, the steel bar at this circumferential location will corrode firstly. Comparing Fig. 13(a) with Fig. 13(b) yields that the chloride ion concentration of concrete pipeline increases significantly as the thickness of concrete protective cover decreases, as the earth pressure and the circumferential position are determined. For example, when the vertical earth pressure, $G_v = 360$ kPa, and the lateral earth pressure, $G_h = 180$ kPa, the chloride ion concentration increases 1.27 folds (from 0.18 to 0.41) as the thickness of concrete protective cover decreases by 25% (from 60 mm to 45 mm). This can be attributed to that with the decrease of concrete protective cover thickness, the diffusion path of chloride ions becomes shorter. Correspondingly, the time requested for the chloride ions arriving at the critical concentration at the steel bar reduces at a certain diffusion rate. Therefore, in the same exposure period, the chloride ion concentration is higher at the steel bar with the smaller thickness of concrete cover. Moreover, it can be found that with as the earth pressures increase, the chloride ion concentration increases significant at the direction of angle $\theta = 0$, while the chloride ion concentration decreases gradually at the direction of angle $\theta = \pi/2$. This is because the variation of earth pressure has a significant effect on the chloride diffusion coefficient in the tensile zone. In addition, the chloride ions diffuse from the outside in, which leads to that the variation of diffusion coefficient has more important effect on the chloride diffusion in the outer layer, compared with that in the inner layer. Comparing Fig. 13(a) with Fig. 13(c) gives that when the underground concrete pipeline is subjected to earth pressures with strong nonuniformity, the chloride ions show a

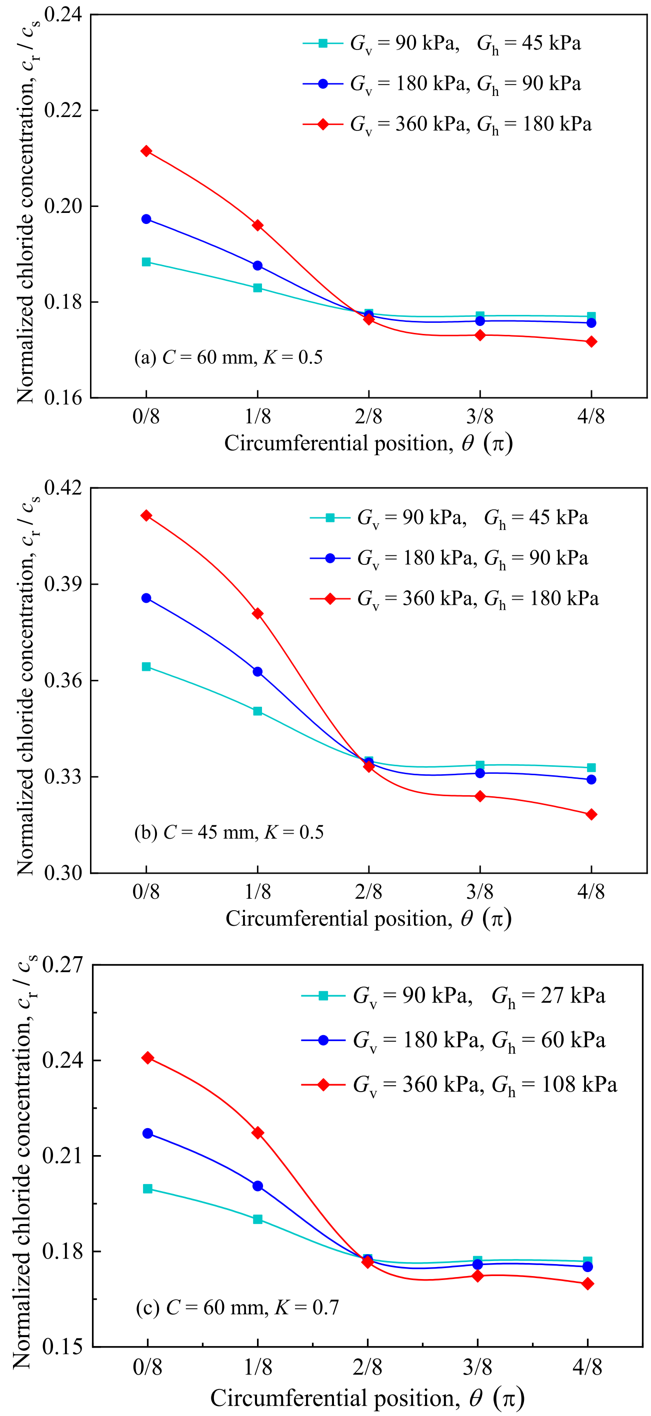

Fig. 13. Chloride ion concentration at steel bar with different cover thicknesses, nonhomogeneous coefficients of earth pressure and earth pressures at different circumferential positions: (a) $C = 60$ mm, $K = 0.5$; (b) $C = 45$ mm, $K = 0.5$ and (c) $C = 60$ mm, $K = 0.7$.

higher concentration at the steel bar. The reason for this phenomenon is that when the pipeline is subjected to uniformly distributed earth pressures, the circumferential stress in the pipeline is the compressive stress and the occurrence of tensile stress is just because of the nonuniformity of earth pressures. Therefore, with the increase of nonuniformity of earth pressures, the maximum value of tensile stress will increase and the tensile zone will develop further as well. As such, the diffusivity of chloride ions will be enhanced and thus the chloride ion concentration

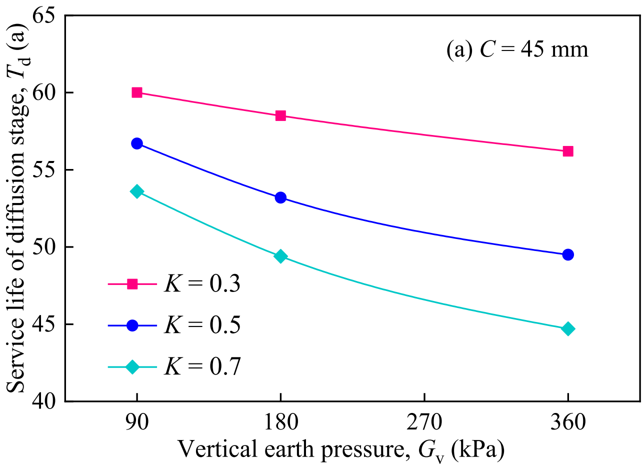

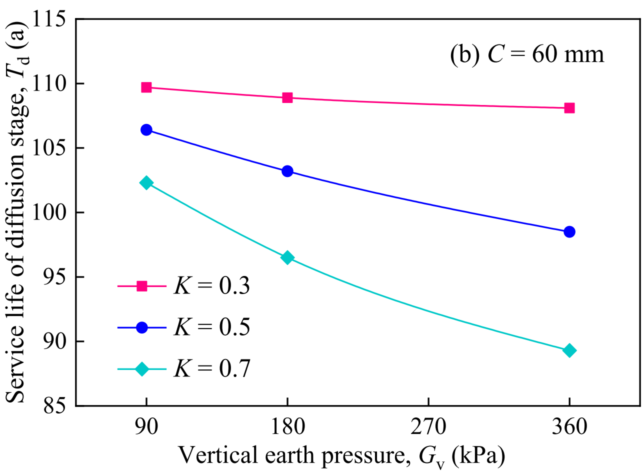

Fig. 14. Service life of pipeline with different vertical earth pressures, nonhomogeneous coefficients of earth pressure and cover thicknesses in the diffusion period: (a) $C = 45$ mm and (b) $C = 60$ mm.

at the steel bar will increase, because of the nonuniformly distributed earth pressures.

Fig. 14 exhibits the effects of thickness of concrete protective cover and nonuniformity of earth pressures on the pipeline service life in the diffusion period. It is observed that the service life decreases with the increase of magnitude of vertical earth pressure and the nonhomogeneous coefficient of earth pressure, while the service life increases with the increase of thickness of concrete cover. It is well known that compared with the hard clay, the soft clay has a larger coefficient of earth pressure at rest. Thus, it has a smaller nonhomogeneous coefficient of earth pressure and correspondingly its nonuniformity is relative weak. As a result, the concrete pipeline buried in such soils has a longer service life. This also illustrates that to extend the pipeline service life, the factors including the buried depth, soil type and thickness of concrete protective cover should be comprehensively considered. In other words, shallow buried depth, thick concrete protective cover and soft clay layer should be prioritized to improve the durability of underground concrete pipeline during diffusion.

5.2. Pipeline service life of corrosion period

In this case analysis, the values of soil weight, mechanical parameters of concrete and initial nonhomogeneous coefficient of earth pressure are all the same as the last case. The other parameters requested to be clarified include: the ion mass proportion in the corrosion products, δ, taken as 0.523; the thickness of porous zone, d_0, equal to 12.5 μm; and the densities of corrosion products, ρ_c, and steel bar, ρ_{st}, equal to 3.6 g/m^3 and 7.9 g/m^3, respectively. Using these parameters, the pipeline service life in the period of corrosion is estimated.

Fig. 15 exhibits the variation of circumferential stress at the inner surface of underground concrete pipeline at different circumferential positions. The pipeline is assumed to be subjected to the vertical earth pressure, G_v, equal to 90 kPa, and the lateral earth pressure,G_h, equal to 9 kPa, as well as the corrosion expansion pressure, P_r, equal to 0.3 MPa. It is found that the circumferential stress varies periodically with the circumferential position and the period is π. When the circumferential position θ equals $\pi/2$ and $3\pi/2$, the circumferential stress is the tensile stress and arrives at its maximum value. Therefore, the tensile stress at the circumferential positions $\theta = \pi/2$ and $\theta = 3\pi/2$ of inner surface of concrete protective cover will reach the tensile strength of concrete at first. In other words, these two positions are the most dangerous position where the cracking may first occur.

Fig. 16 shows the prediction on pipeline service life in the corrosion period, which is assumed to be subjected to different nonuniformly distributed earth pressures and have different concrete protective cover thicknesses. It can be found that with the same nonhomogeneous coefficient of earth pressure and concrete protective cover thickness, the service life reduces obviously with the increase of nonuniformly distributed earth pressures. This is because the larger nonuniformly distributed earth pressure results in a larger circumferential stresses at the dangerous surface (dangerous surface means the surface where the cracking is easiest to occur) and as such the circumferential stress only needs the superposition of a very little corrosion expansion pressure to reach the tensile strength of concrete for cracking. This further indicates that only a few corrosion products can yield the cracking of underground concrete pipeline. Therefore, its corresponding time for corrosion becomes shorter, which indicates that the underground concrete pipeline has a shorter service life in the corrosion period.

Comparing Fig. 16(a) with Fig. 16(b) yields that with the same concrete protective cover thickness and vertical earth pressure, the smaller nonhomogeneous coefficient of earth pressure corresponds to a longer pipeline service life. The reason is that the stress in the pipeline tends to be the compressive stress when the nonuniformity of earth pressure is weak. As such, the circumferential tensile stress reduces at the dangerous surface and even turns into the compressive stress as the nonhomogeneous coefficient of earth pressure is equal to zero. As a consequence, a larger corrosion expansion pressure is required to give rise to the cracking of

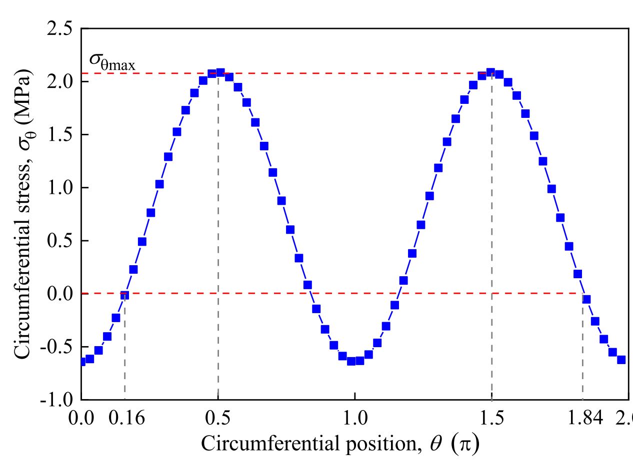

Fig. 15. Circumferential stress at inner surface of concrete cover subjected to corrosion expansion pression at different circumferential positions.

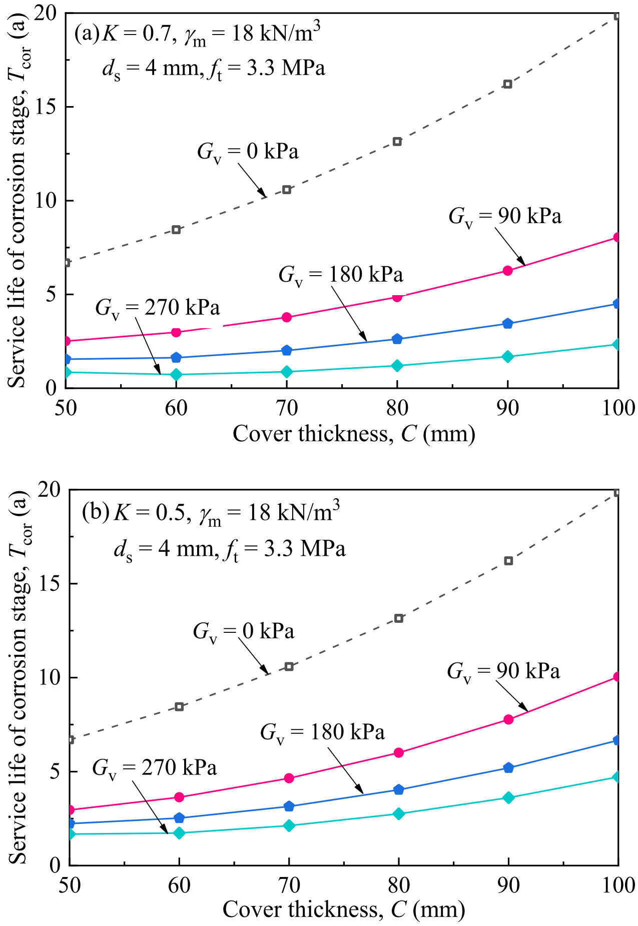

Fig. 16. Service life of pipeline with different cover thicknesses and nonuniformly distributed earth pressures in corrosion period.

pipeline, which accounts for that the pipeline service life is extended under such conditions.

Moreover, it can be observed that when the nonuniformly distributed earth pressure is determined, the pipeline service life increases as the concrete protective cover thickness increases. This can be attributed to that the inner radius of outer protective cover increases due to the increase of cover thickness. This implies that more corrosion products require to be produced to fill in porous zone and to yield the same corrosion expansion pressure. Correspondingly, more corrosion products mean a long-time corrosion and hence the pipeline service life is extended. Hence, when designing underground concrete pipelines, shallow buried depth, large concrete protective cover thickness and soft clay layer should be given priority to ensure that the underground concrete pipeline can meet the use requirement in the whole service period.

6. Conclusions

In this paper, the service life of concrete pipelines subjected to nonuniformly distributed earth pressures in chloride contaminated soils has been predicted by estimating the service life in the diffusion and corrosion periods, respectively. In both periods, the effects of nonuniformly distributed earth pressures have been taken into account by incorporating the solution to the stress distribution in the pipeline derived on the basis of the principle of linear superposition. The chloride diffusion in the pipeline was simulated based on the diffusion model for a dual compound media and the prediction on service life of this period was examined by ABAQUS simulations. The service life during corrosion was predicted with the help of corrosion expansion pressure along with the concrete tensile strength and the mechanical analysis of pipeline. The effects of nonuniformly distributed earth pressures and concrete protective cover thickness were explored by comprehensive parametric studies.

The conclusions drawn from this study indicate that because of the effects of nonuniformly distributed earth pressures, the stress state and stress level within the underground concrete pipeline vary from location to location, which is different from those in the pipelines subjected to uniformly distributed earth pressures. In addition, at the same radial location, the circumferential stress varies periodically from the tensile stress to the compressive stress or vice visa along the circumferential direction. However, the compressive stress takes the dominant place no matter in the radial direction or in the circumferential direction. During the chloride diffusion in the pipeline, the maximum chloride ion concentration around steel bars reduces remarkably as the increase of concrete protective cover thickness, while it increases with the increase of stress level and nonuniformity of nonuniformly distributed earth pressures. Thicker concrete protective cover, shallower buried depth and soft clay layer should be given priority to when designing concrete pipelines buried in chlorinated soils, so as to ensure that underground concrete pipelines have an adequate service life.

CRediT authorship contribution statement

Lin Li: Conceptualization, Methodology, Software, Writing - review & editing. **Weibing Gong:** Software, Methodology, Data curation, Writing - original draft. **Jingpei Li:** Conceptualization, Supervision, Funding acquisition, Writing - review & editing.

Declaration of Competing Interest

The authors declare that they have no known competing financial interests or personal relationships that could have appeared to influence the work reported in this paper.

Acknowledgment

This study was supported by the National Natural Science Foundation of China with Grant No. 41772290.

Appendix. The expressions of parameters E_{jn} ($j = 2, 3$) and F_{kn} ($k = 1, 2, 3$) are as follows

$$F_{1n} = -\frac{J_1\left(\frac{r_1\beta_n}{\sqrt{D_1}}\right)}{Y_1\left(\frac{r_1\beta_n}{\sqrt{D_1}}\right)} \tag{A1}$$

$$E_{2n} = -\frac{\sqrt{\frac{D_1}{D_2}}\left[J_1\left(\frac{r_2\beta_n}{\sqrt{D_1}}\right) + F_{1n}Y_1\left(\frac{r_2\beta_n}{\sqrt{D_1}}\right)\right] - F_{2n}Y_1\left(\left(\frac{r_2\beta_n}{\sqrt{D_2}}\right)\right)}{J_1\left(\frac{r_2\beta_n}{\sqrt{D_2}}\right)} \tag{A2}$$

$$F_{2n} = \frac{J_1\left(\frac{r_2\beta_n}{\sqrt{D_2}}\right)\left[J_0\left(\frac{r_2\beta_n}{\sqrt{D_1}}\right) + F_{1n}Y_0\left(\frac{r_2\beta_n}{\sqrt{D_1}}\right)\right] - \sqrt{\frac{D_1}{D_2}}J_0\left(\frac{r_2\beta_n}{\sqrt{D_2}}\right)\left[J_1\left(\frac{r_2\beta_n}{\sqrt{D_1}}\right) + F_{1n}Y_1\left(\frac{r_2\beta_n}{\sqrt{D_1}}\right)\right]}{Y_0\left(\frac{r_2\beta_n}{\sqrt{D_2}}\right)J_1\left(\frac{r_2\beta_n}{\sqrt{D_2}}\right) - Y_1\left(\frac{r_2\beta_n}{\sqrt{D_2}}\right)J_0\left(\frac{r_2\beta_n}{\sqrt{D_2}}\right)} \tag{A3}$$

$$E_{3n} = -\frac{\sqrt{\frac{D_2}{D_3}}\left[E_{2n}J_1\left(\frac{r_3\beta_n}{\sqrt{D_2}}\right) + F_{2n}Y_1\left(\frac{r_3\beta_n}{\sqrt{D_3}}\right)\right] - F_{2n}Y_1\left(\left(\frac{r_3\beta_n}{\sqrt{D_3}}\right)\right)}{J_1\left(\frac{r_3\beta_n}{\sqrt{D_3}}\right)} \tag{A4}$$

$$F_{3n} = \frac{J_1\left(\frac{r_3\beta_n}{\sqrt{D_3}}\right)\left[E_{2n}J_0\left(\frac{r_3\beta_n}{\sqrt{D_2}}\right) + F_{2n}Y_0\left(\frac{r_3\beta_n}{\sqrt{D_2}}\right)\right] - \sqrt{\frac{D_2}{D_3}}J_0\left(\frac{r_3\beta_n}{\sqrt{D_3}}\right)\left[E_{2n}J_1\left(\frac{r_3\beta_n}{\sqrt{D_2}}\right) + F_{2n}Y_1\left(\frac{r_3\beta_n}{\sqrt{D_2}}\right)\right]}{Y_0\left(\frac{r_3\beta_n}{\sqrt{D_3}}\right)J_1\left(\frac{r_3\beta_n}{\sqrt{D_3}}\right) - Y_1\left(\frac{r_3\beta_n}{\sqrt{D_3}}\right)J_0\left(\frac{r_3\beta_n}{\sqrt{D_3}}\right)} \tag{A5}$$

where r_i $(i = 1, 2, 3)$ is the radius of the ith layer of compound media; and J_0 and Y_0 are the zero-order first kind and second kind Bessel functions, respectively.

References

[1] S.W. Tang, Y. Yao, C. Andrade, Z.J. Li, Recent durability studies on concrete structure, Cem. Concr. Res. 78 (2015) 143–154.

[2] C. Medina, M.S. De Rojas, C. Thomas, J.A. Polanco, M. Frías, Durability of recycled concrete made with recycled ceramic sanitary ware aggregate. Inter-indicator relationships, *Constr. Build. Mater.* 105 (2016) 480–486.

[3] H. Yu, B. Da, H. Ma, H. Zhu, Q. Yu, H. Ye, X. Jing, Durability of concrete structures in tropical atoll environment, Ocean Eng. 135 (2017) 1–10.

[4] L. Basheer, J. Kropp, D.J. Cleland, Assessment of the durability of concrete from its permeation properties: a review, Constr. Build. Mater. 15 (2–3) (2001) 93–103.

[5] X. Shi, N. Xie, K. Fortune, J. Gong, Durability of steel reinforced concrete in chloride environments: an overview, Constr. Build. Mater. 30 (2012) 125–138.

[6] S.J. Kwon, U.J. Na, S.S. Park, S.H. Jung, Service life prediction of concrete wharves with early-aged crack: probabilistic approach for chloride diffusion, Struct. Saf. 31 (1) (2009) 75–83.

[7] A.A. Jee, B. Pradhan, Study on development of empirical relationships between durability parameters of concrete made with different types of binder and exposed to chloride environment, Constr. Build. Mater. 212 (2019) 799–817.

[8] A. Konin, R. Francois, G. Arliguie, Penetration of chlorides in relation to the microcracking state into reinforced ordinary and high strength concrete, Mater. Struct. 31 (5) (1998) 310–316.

[9] R. Francois, J.C. Maso, Effect of damage in reinforced concrete on carbonation or chloride penetration, Cem. Concr. Res. 18 (6) (1988) 961–970.

[10] N. Gowripalan, V. Sirivivatnanon, C.C. Lim, Chloride diffusivity of concrete cracked in flexure, Cem. Concr. Res. 30 (5) (2000) 725–730.

[11] A. Castel, R. Francois, G. Arliguie, Chloride diffusion in reinforced concrete beam under sustained loading, ACI Special Publication 200 (2001) 647–662.

[12] C.C. Lim, N. Gowripalan, V. Sirivivatnanon, Microcracking and chloride permeability of concrete under uniaxial compression, Cem. Concr. Compos. 22 (5) (2000) 353–360.

[13] C.H. Lu, H.L. Wang, W.L. Jin, Modeling the influence of stress level on chloride transport in prestressed concrete, International Conference on Durability of Concrete Structures, Hangzhou, China 26 (2008) 239–245.

[14] J. Zheng, X. Zhou, Analytical solution for the chloride diffusivity of hardened cement paste, J. Mater. Civ. Eng. 20 (5) (2008) 384–391.

[15] Q. Huang, Calculation of Underground Pipeline, Hubei Science & Technology Press, Wuhan, China, 1987 (in Chinese).

[16] H. Li, Experiments on Chloride Penetration in Concrete and Prediction on Service Life of Power Transmission and Transformation Foundation. Master thesis, Tongji University, 2016 (in Chinese).

[17] M. Boulfiza, K. Sakai, N. Banthia, H. Yoshida, Prediction of chloride ions ingress in uncracked and cracked concrete, ACI Mater. J. 100 (1) (2003) 38–48.

[18] H. Wang, J. Li, L. Li, H. Chen, Service life of underground concrete pipeline with original incomplete cracks in chlorinated soils: theoretical prediction, Constr. Build. Mater. 188 (2018) 1166–1178.

[19] W. Shao, J. Li, Service life prediction of cracked RC pipe piles exposed to marine environments, Constr. Build. Mater. 64 (2014) 301–307.

[20] Y. Liu, Modeling the time-to corrosion cracking of the cover concrete in chloride contaminated reinforced concrete structures. Doctoral dissertation, Virginia Tech, 1996.

[21] T. Reale, A. O'Connor, A review and comparative analysis of corrosion-induced time to first crack models, Constr. Build. Mater. 36 (2012) 475–483.

[22] Y. Wang, Y. Tang, C. Chen, L. Yang, Study on life predicting model of subsea tunnel based on chloride corrosion, Struct. Eng. 28 (4) (2012) 57–62 (in Chinese).

[23] A. Djerbi, S. Bonnet, A. Khelidj, V. Baroghel-Bouny, Influence of traversing crack on chloride diffusion into concrete, Cem. Concr. Res. 38 (6) (2008) 877–883.